

Thermal desorption and IR spectrometric investigation of polyamorphic and polymorphic transformations in cryovacuum condensates of water

A. Drobyshev, A. Aldiyarov, D. Zhumagaliuly, V. Kurnosov, and N. Tokmoldin

Citation: *Low Temperature Physics* **33**, 472 (2007); doi: 10.1063/1.2737563

View online: <http://dx.doi.org/10.1063/1.2737563>

View Table of Contents: <http://scitation.aip.org/content/aip/journal/ltp/33/5?ver=pdfcov>

Published by the [AIP Publishing](#)

Articles you may be interested in

[Transformation of cryovacuum condensates of ethanol near the glass transition temperature](#)

Low Temp. Phys. **39**, 714 (2013); 10.1063/1.4818634

[Fast scanning calorimetry studies of the glass transition in doped amorphous solid water: Evidence for the existence of a unique vicinal phase](#)

J. Chem. Phys. **138**, 084501 (2013); 10.1063/1.4789629

[Deposition and crystallization studies of thin amorphous solid water films on Ru\(0001\) and on CO-precovered Ru\(0001\)](#)

J. Chem. Phys. **127**, 094703 (2007); 10.1063/1.2770726

[Thermally stimulated transformations in cryovacuum water ices](#)

Low Temp. Phys. **33**, 355 (2007); 10.1063/1.2720084

[On the role of frustration on the glass transition and polyamorphism of mesoscopically heterophase liquids](#)

J. Chem. Phys. **125**, 064503 (2006); 10.1063/1.2238858



Thermal desorption and IR spectrometric investigation of polyamorphic and polymorphic transformations in cryovacuum condensates of water

A. Drobyshev,^{a)} A. Aldiyarov, D. Zhumagaliuly, V. Kurnosov, and N. Tokmoldin

Al-Farabi Kazakh National University, Tole bi 96, Almaty 480012, Kazakhstan

(Submitted September 5, 2006; revised November 27, 2006)

Fiz. Nizk. Temp. **33**, 627–638(May 2007)

Simultaneous thermal desorption and IR spectrometric studies of thermally stimulated transformations in thin films of cryovacuum condensates of water are carried out. It is shown that the temperature interval 12–36 K is the existence region of a high-density form of amorphous solid water. The transition of amorphous high-density ice to a low-density amorphous state starts at $T \approx 39$ K and is completed in the temperature region 60–70 K. This process is accompanied by pore formation and reaches its maximum intensity at $T \approx 42$ K. The transition temperature from the glassy amorphous ice to a super-viscous liquid state is determined: $T_g = 137 \pm 2$ K. Further increase in temperature leads to transformations of a stepped character in the layer. This may be due to competing processes of crystallization via the growth of cubic and hexagonal nuclei and also to direct crystallization of the super-viscous liquid water formed at T_g and existing together with the crystalline phase up to temperatures ~ 200 K. Anomalous behavior of the sample at temperatures preceding sublimation is revealed. This confirms that a multicomponent system consisting of amorphous and crystalline samples has different values of the equilibrium pressures of the gas phase, corresponding to partial activation energies of sublimation, i.e., at high temperatures amorphous water evaporates at an earlier stage, and then recondenses on the crystalline components. © 2007 American Institute of Physics. [DOI: [10.1063/1.2737563](https://doi.org/10.1063/1.2737563)]

I. INTRODUCTION

The present state of research on polyamorphic and polymorphic cryovacuum condensates of solid water is that there is an enormous volume of experimental and theoretical/computational data, often contradictory. In every case the generally recognized points of agreement are much fewer than the points of contention.^{1–5} Among the points in common is the obvious recognition of the fact that the properties of the ices formed depend on the conditions of their formation and existence: the substrate temperature and morphology, the rates of condensation and warming of the samples, the composition of the gas phase (directed condensation or growth from spatially uniform gaseous phase), and the film thickness.^{6–8}

The low-temperature form of cryovacuum condensates of water (ASW) in the course of a gradual warming undergoes a transition to a state of super-viscous liquid state (Water A). Is “Water A” an independent condensed state of water, or is it the final link in a continuous sequence of states: water–supercooled water–“Water A”?^{9–12} The answer to this fundamental question should be given by studies of the structure of the amorphous forms of water and their transformations. The key issues in the debate can be characterized as follows.

1. Is there a low-temperature high-density form (hda) of ASW ($\rho = 1.07$ g/cm³) formed in the course of gas-phase cryodeposition at substrate temperatures below 30 K? Such a phase was hypothesized first, apparently, by A. H. Narten for epitaxial layers with a condensation temperature below 10 K.⁸ It was later shown^{1–3,9} that hda is formed on a substrate at a temperature of 15 K and exists up to a temperature of 38 K. Further increase of temperature to 70 K leads to a

gradual transition of the high-density ice to the so-called low-density amorphous ice (lda), with $\rho = 0.94$ g/cm³. Although the experimental information supporting these conclusions is of good quality, it has been continually subjected to critical analysis. In particular, in Ref. 13 as a result of investigations and modeling of vacuum-condensed amorphous ices, it was concluded that there is no proof that hda is formed at very low condensation temperatures. Meanwhile, it has been shown that the angular distortions of the network of hydrogen bonds for amorphous low-temperature layers of water are similar to the corresponding distortions upon the amorphization of crystalline ices under pressure, which results in the formation of high-density ices. Thus the existence of high-density low-temperature cryovacuum condensates of water is still an open question.

2. Is the thermally stimulated sequence of polyamorphic transformations in ASW a discrete process, with definite values of the transformation temperatures, or is the amorphous form of water a continuous sequence of gradually varying states? From the known dependence of the properties of ASW on the conditions of formation, it is assumed^{1–4} that there exists a finite set of states differing in the structure of the short-range order, each with its own existence region in temperature. Meanwhile, recent structural studies of the metastable forms of amorphous ices attest to the existence of a large number of amorphous forms of ASW. In particular, in Ref. 14 the neutron and x-ray diffraction methods were used to investigate at least five different amorphous states, and the existence of an even greater number was proposed. The authors reasonably assume that a continuous distribution of reversible forms may exist between the hda and lda states.

3. What is the value of the glass transition temperature T_g ? Numerous experimental studies, e.g., by differential scanning calorimetry,^{15–17} have found a glass point T_g of around 136 K with a standard deviation of 2 kelvin. However, there also exist studies that give a different interpretation of the experimental data.^{18,19} Their critical analysis of the value of T_g is based on the known fact that an exothermic process of crystallization and an endothermic transition from the glassy state to the super-viscous liquid state take place in the same, rather narrow temperature interval and overlap each other. There are widely used methods for separating the experimental data, one of these being isothermal annealing of the samples. Nevertheless, the debates continue,²⁰ and the question cannot be considered closed, although the majority view tends toward recognition of a glass transition temperature of 136 K.⁵

4. What are the thermodynamic boundaries of the existence of “Water A” from the glass point to the crystallization temperature? This question is intimately related to the question of the structure of the ASW and how does it affect the kinetic relationships observed in the polyamorphic and polymorphic transformations and sublimation processes. It is the relationship between the crystalline and amorphous forms in a sample that largely determines its behavior, especially at temperatures much higher than T_g . In a number of papers^{3,21} an important role is ascribed to the difference of the activation energies for sublimation of the amorphous and crystalline constituents in the process of sublimation of water ices, and in the existence region of the crystalline (cubic) ices a material in the form of a super-viscous liquid is present, which exists to temperatures above 200 K. Not only are studies of this kind of fundamental value for research in the physics and chemistry of ice, but there are also obvious astrophysical applications for understanding processes occurring on the water-bearing surfaces of natural cosmic objects.

II. EXPERIMENT

Statement of the problem

The concepts set forth above are obviously open to question, but they do provide a serious conceptual basis for continuing detailed experiment research on processes of thermally stimulated transformations in cryovacuum condensates of water. The essence of our investigations is as follows (the experimental setup will be described in more detail in a separate Section). A thin water cryocondensate film is deposited on a metallic mirror (silvered copper substrate) placed on the upper flange of a microcryogenic system. The condensation temperature is varied from $T=12$ K on up. The condensation pressure was set by a leak in the interval 10^{-6} – 10^{-4} torr. Thus a scheme with a spatially uniform angular distribution of the water molecules incident on the substrate was realized (background condensation). The thickness of the film, its refraction coefficient, and the rate of condensation were measured with the aid of a double-beam laser interferometer. The film thickness was 0.5–10 μm , permitting measurements at higher temperatures. After measurement of the IR reflection spectra at the cryodeposition temperature a gradual heating of the substrate was begun, with simultaneous measurement of the chosen parameters.

The conventional scheme of the experiment, condensation–analysis–warming–analysis, affords the following possibilities:

1. Continuous measurement of a chosen parameter by at least two independent methods. This makes it possible to determine precisely the temperature intervals of the existence and transformations of the polyamorphic and polymorphous states of ice.

2. Methodical separation of processes occurring in parallel in the samples, such as exothermic crystallization and endothermic vitrification. Thus the use of a differential scanning calorimeter^{15–17} yields rich information, but studies of this nature in the vicinity of the glass transition T_g inevitably require intervention in the natural thermally stimulated processes of transformations in ASW. This intervention consists in a preliminary warming of the sample, which is not completely correct to do, since it levels out features acquired by the films during cryodeposition, which can form the dominant pathway for relaxation processes in the investigated cryovacuum condensates.^{1,2}

3. The possibility of making measurements by the same method over a wide temperature interval—from condensation to sublimation.

Measurement techniques

In accordance with the statement of the problem and the requirements on the methods of measurement during the growth and warming of the film the following quantities were measured.

1. The growth rate, thickness, and refractive index of the cryodeposits, measured with a dual-beam laser interferometer.

2. The variation of the IR spectrometer signal at a fixed observation frequency. The observation frequency was 3015 cm^{-1} —the low-frequency edge of the absorption band of the O–H bond. Our numerous previous studies^{22–24} had shown that this region of the spectrum (together with the librational oscillations) is extremely sensitive to changes in the polymorphic and polyamorphic states of the film.

3. The thermal desorption pressure variation in the vacuum chamber during warming. In our measurements we did not use a mass spectrometer, as there was reason to assume that the main component collected at the surface of the pores of the ASW would be nitrogen. This is confirmed by the fact that a sharp increase of the vacuum in the chamber is observed when the temperature of the cryopanel of the pump reached approximately $T=23$ – 24 K, and specifically for nitrogen in this temperature interval the equilibrium pressure decreases from $\approx 10^{-7}$ torr to $\approx 10^{-8}$ torr.²⁵

A further goal was to use this method for determination of the boundaries of the existence regions of the modifications of solid water. For this we measured the integrated pressure in the vacuum chamber and its variation due to desorption of nitrogen molecules in the course of the polyamorphic and polymorphic transformations.

4. The reflectance of the substrate with the film of water cryocondensate, at the frequency of the He–Ne laser (638 nm). This method has been used for analysis of the change of morphology of the film surface during heating.

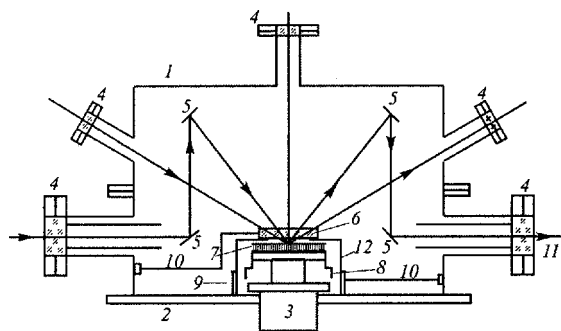


FIG. 1. Diagram of the vacuum chamber of the experimental setup and measurement cell: 1—case of vacuum chamber, 2—base of vacuum chamber, 3—McMahon microrefrigerator, 4—optical window, 5—optical waveguide, 6—KBr shielding slab, 7—substrate, 8—cryopump, 9—slide valve, 10—magnetic servo, 11—KBr optical window, 12 protective cowl.

and also for monitoring possible parasitic condensation (or recondensation) of water during the warming.

5. Measurement of the IR reflection spectra at fixed temperatures of the substrate with the sample. These measurements were made periodically to establish the interrelationship between variables of the interferometer signal at frequency 3015 cm^{-1} and the character of the variation of the IR spectrum.

The simultaneous use of IR spectrometric and thermal desorption methods permits a more reliable interpretation of the results obtained. Furthermore, such an approach makes it possible to reveal features of the warming curve that had previously been ascribed to measurement error.

Experimental setup

The experimental setup on which the measurements were made has been described repeatedly and in detail (see, in particular, Ref. 22). However, for studying the thermally stimulated transformations in ASW the setup was upgraded mainly to improve the stability of the conditions during measurements. A diagram of the experimental setup is shown in Fig. 1. A retractable KBr slab (6) could be placed over the substrate by means of a magnetic servo (10) to cover the working surface (7) to prevent uncontrolled precondensation and to shield it from secondary processes in the course of the warming. The distance between the substrate and shield was 5 mm.

Furthermore, additional copper plates (8) were placed on the surface of the cold, upper flange of the McMahon microrefrigerator to serve as cryocondensation pumps. For the cryopumping the protective cowl (12) had apertures that could be closed with cylindrical slide valves (9) driven by magnetic servos (10). This made it possible to raise the base level of vacuum in the chamber to 5×10^{-8} torr. Moreover, shielding the substrate with the retractable slab and the protective cowl creates a closed volume around the substrate where the pressure is much lower than the pressure in the outer vacuum chamber. The use of a KBr slab as a shield permits making measurements over a wide IR range without disrupting these conditions.

The main working parameters of the experimental setup and equipment are as follows:

- dimensions of the vacuum chamber: a cylinder with diameter and height equal to 450 mm (stainless steel);
- diameter of the upper flange of the vacuum chamber: 60 mm; diameter of the working surface: 40 mm (silvered copper substrate);
- highest vacuum in the chamber: 5×10^{-8} torr (zeolite and magnetic discharge pumps, condensation pump);
- minimum substrate temperature: 12 K (McMahon refrigerator). The temperature is measured with a thermocouple (Au+0.07% Fe)—Cu with an accuracy of 0.5 kelvin or better in the low-temperature region;
- range of the IR spectrometer: $400\text{--}4200\text{ cm}^{-1}$ (IKS-29);
- film thickness interval: $0.2\text{--}20\text{ }\mu\text{m}$ (dual-beam laser interferometer).

Order in which experiments are done

After the vacuum chamber was pumped down with the zeolite and magnetic discharge pumps to a pressure of 10^{-6} torr, the condensation surface was covered by a KBr slab and the microcryogenic system (3) was turned on. As the upper flange was cooled, the vacuum in the chamber improved as a result of cryopumping and equalled 5×10^{-8} torr at $T=16\text{ K}$. Then the vacuum chamber was closed off from the pumping system, including the cryopump. After this the shielding slab (6) was retracted by means of a magnetic servo, and water vapor was admitted to the chamber through a leak. The source of water vapor was twice-distilled liquid water held in an ampoule placed directly on the case of the admitting valve. The pressure in the chamber was raised to the experimental values (in the interval $10^{-6}\text{--}10^{-4}$ torr) and a sample of a specified thickness was condensed on the substrate (the thickness was monitored by a laser interferometer). The water vapor leak was shut off, and the discharge valve of the magnetic discharge pumps and the door of the cryopump (9) were opened. A vacuum of 10^{-7} torr or better was established. Then, depending on the task, the substrate was left uncovered or was covered by the slab (6).

The IR reflection spectrum was measured at a fixed substrate temperature. A temperature above 16 K was maintained with the aid of a heater. All of the measurements were made in an automatic mode with the use of an E14-140 analog-to-digital converter. This applies to all the subsequent measurements as well.

After measurement of the IR spectra, the spectrometer was set to a frequency of 3015 cm^{-1} and simultaneous measurements of the variations of the signals from the interferometer, vacuum meter, and laser interferometer were made in the course of warming the sample with the microcryogenic system turned off. The rate of warming of the samples was $V_{\text{ann}} \approx 0.03\text{ K/s}$ in the temperature interval 16–60 K and $V_{\text{ann}} \approx 0.01\text{ K/s}$ at temperatures of 60 K and above. When the substrate reached temperatures of over 165 K, to prevent intense evaporation of the sample the outpumping of the chamber was shut off and the subsequent measurements were made at the equilibrium pressure of the gas phase.

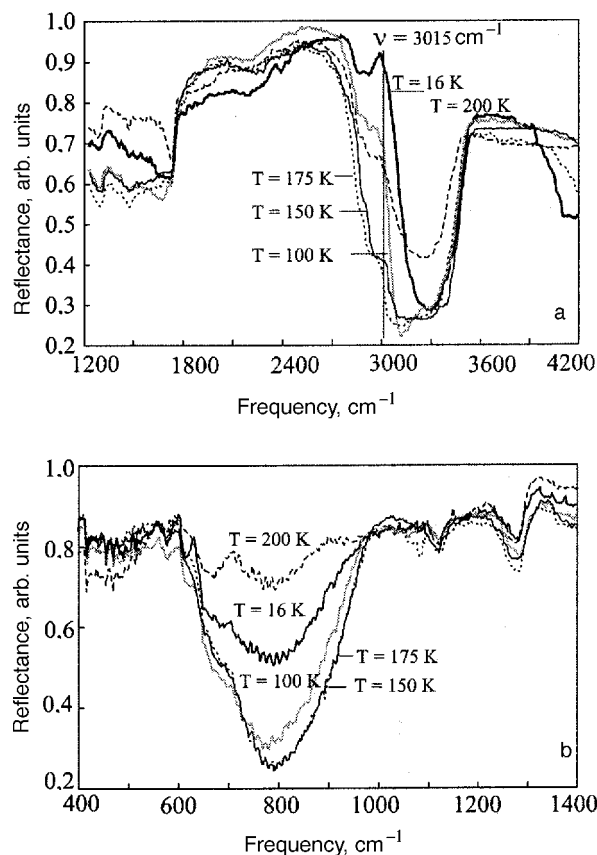


FIG. 2. IR spectra of ASW film and crystalline samples at different temperatures in the frequency intervals [cm⁻¹]: 1200–4200 (a), 400–1400 (b).

III. RESULTS

The goal of these studies was to make continuous measurements of selected parameters whose variation is correlated with polyamorphic and polymorphic transformations in an ASW film in the course of its warming. There is a well-known relationship between the shape and position of the absorption peak of the O–H bond and the degree of hydrogen bonding of the water molecules, which is determined by the structural state of the ice. One of the most widely used tools for analysis of the processes occurring in various physical systems is IR spectrometry. Here, as in many of our previous studies, we supplement this method with measurements at a fixed frequency of the IR spectrometer. The combination of these methods gives an idea of the changes in the character and position of the bands of stretching vibrations and provides a continuous picture of these changes.

Figure 2 shows the IR spectra of an ASW sample 0.75 μm thick, deposited at a temperature of 16 K and then warmed to temperatures of 100, 150, 175, and 200 K, at which temperatures the system the temperature-stabilizing system was turned on. The film thickness was $d=0.75\text{ }\mu\text{m}$, the condensation temperature $T=16\text{ K}$, and the rate of warming $V_{\text{ann}}\approx 0.03\text{ K/s}$ in the interval 16–60 K and $V_{\text{ann}}\approx 0.01\text{ K/s}$ at $T>60\text{ K}$. In Fig. 2a we have drawn a line of constant frequency which clearly demonstrates the qualitative variation of the IR spectrometer signal as the sample is warmed.

Figure 2 clearly demonstrates the substantial changes of the character and position of the absorption band that result

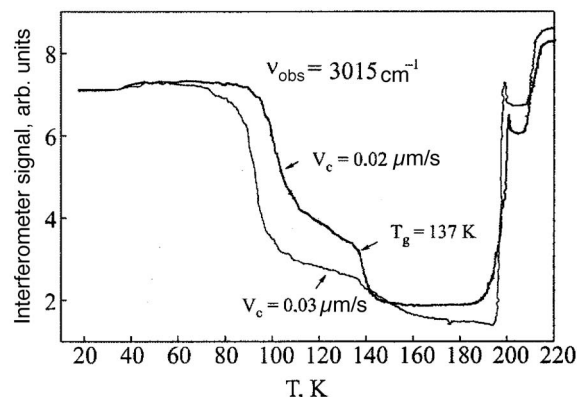


FIG. 3. Variation of the interferometer signal during warming of thin film of ASW of thickness $d=0.75\text{ }\mu\text{m}$, formed at a condensation temperature $T=16\text{ K}$. The observation frequency $\nu_{\text{obs}}=3015\text{ cm}^{-1}$, the warming time $\tau=6\text{ h}$.

from heating of the film and the corresponding transformations in it. The substantial shift of the stretching band of absorption to lower frequencies with increasing temperature indicates an enhancement of the intermolecular interaction via the network of hydrogen bonds. The obvious difference in the ASW_{16 K} and ASW_{100 K} spectra can be interpreted as being due to different amorphous states of solid water.

The IR spectra of the film at temperatures of 150 and 175 K are practically identical and have the largest low-frequency shift. One can with complete justification assume that these samples are found in a crystalline (possibly I_c) state. The slight difference between them has an insignificant effect on the absorption band of the O–H bond (intermolecular interaction), and cannot affect the intramolecular proton tunneling (librations), as is well seen in Fig. 2b.

Further increase of temperature leads to a significant change of the absorption spectrum. At 200 K the absorption band of the O–H bond is shifted to higher frequencies, and the amplitude of the absorption decreases. The decrease in amplitude is clearly due to the partial evaporation of the sample, which is manifested with particular clarity in the libration modes (Fig. 2b). And the shift of the band and the vanishing of the fine structure that is characteristic for crystalline samples is due to processes of reconcondensation of an amorphous–crystalline state owing to the higher pressure of the saturated vapor for the amorphous phase.^{26,27}

Analysis of Fig. 2 leads to the natural desire to determine more precisely the temperatures at which changes are observed and the structural transformations corresponding to them. The results of such measurements are presented in Figs. 3 and 4. However, before turning to a detailed discussion of these results, we note the following. The data presented in Figs. 2 and 4 pertain to a single experiment. We could not measure simultaneously both the IR spectra and the effect of warming at a fixed frequency. Thus Fig. 2 gives only a qualitative idea of the possible changes of the reflection spectra during the warming of the ASW. Furthermore, we carried out special studies of the stability of the heating processes, which showed the following. ASW samples of the same thickness, formed under identical (as far as experimentally possible) conditions, can have a different character of the heating. We assume that this is a consequence of the

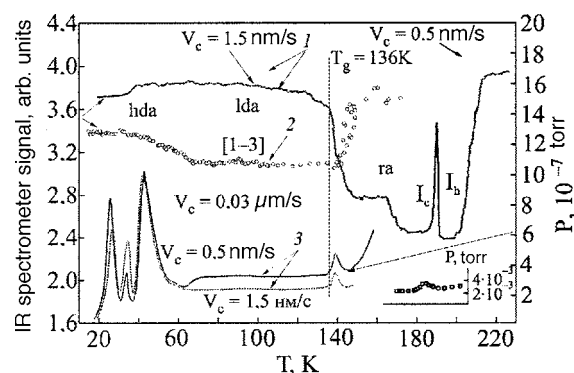


FIG. 4. Variation of the IR spectrometer signal on heating of an ASW film of thickness $d=0.75\ \mu\text{m}$, formed at a condensation temperature $T=16\ \text{K}$. The variation of the signal at frequency $\nu=3015\ \text{cm}^{-1}$ (1); comparison with the data of Refs. 1–3 (2); the thermal desorption curves of ASW (normalized according to the initial pressure $P=10^{-7}$ torr) (3). The inset in the lower right-hand corner shows the variation of the pressure upon a possible recondensation of the amorphous state to a crystalline state.

stochastic character of the formation of the samples at low temperatures, as is indicated by the ratio between the cubic and hexagonal crystals in the “matrix” of amorphous solid water.^{1,2,28}

Figure 3 shows the results of one such experiment, which to a certain degree can be compared with the IR spectra presented in Fig. 2. Despite the closeness of the condensation conditions (the only difference is a slight change of the rate of deposition), the character of the warming in the temperature interval from 60 K to the glass point is different. In the framework of the assumptions and terminology proposed by Jenniskens and co-workers, we can assume that in one of the experiments ($V_c=0.03\ \mu\text{m/s}$) the transition from a low-density amorphous state to the restrained state (ra) begins significantly earlier, and the subsequent transformations occur more smoothly, than for a film formed at a rate of $V_c=0.02\ \mu\text{m/s}$. We are convinced that this circumstance is not a consequence of a difference in the rates of cryodeposition, but we have used the deposition rates as a label to identify the curves in the text. The two curves can be separated provisionally into several temperature intervals, at the boundaries of which the behavior of the samples is the same.

The interval 16–36 K—the interferometer signal is has a constant value, i.e., the absorption band does not change in position or shape.

The interval 40–60 K—there is a weak, gradual increase in signal, which may indicate a slight narrowing of the absorption band.

The interval from 60 K to ≈ 70 –90 K—the sample does not change substantially.

The intervals 90–110 K and 110–135 K correspond to two regimes of shifting of the absorption band to lower frequencies.

$T=137\ \text{K}$ —the transition from the glassy state to super-viscous water.

The interval 142–190 K—the absence of change.

The interval 190–220 K—sublimation–recondensation processes.

The warming curves presented in Fig. 4 differ from the data of Fig. 3 to an even greater degree. However, in the present article we have not compared warming curves ob-

tained under approximately equal experimental conditions. These studies were presented in Ref. 29. Here we focus on an analysis of data on the thermally stimulated transformations in ASW obtained simultaneously by differential methods of measurement.

Thus in Fig. 4 we present data obtained in the course of warming of asw samples condensed at a substrate temperature of 16 K in the “background condensation” mode. The results of two experiments are shown, differing in the rate of cryocondensation. The samples were $0.75\ \mu\text{m}$ thick. The two upper curves reflect the variation of the IR spectrometer signal at a frequency of $3015\ \text{cm}^{-1}$ (left-hand scale). The lower curves correspond to the upper curves of the variation of the pressure in the vacuum chamber in the course of the warming of the samples (right-hand scale; the data are normalized according to the initial pressure in the chamber, equal to 10^{-7} torr at $T=16\ \text{K}$). In the inset in the lower right-hand corner we show the variation of the pressure in the chamber at high temperatures preceding sublimation of the sample. All of the data were obtained for an open substrate, i.e., with the shielding slab of KBr in the retracted position (Fig. 1). At the center, for comparison, we show the results of studies done by Jenniskens and co-workers in Refs. 1–3 (the left-hand scale, in arbitrary units). The abbreviations hda, lda, ra, I_c , and I_h denote the approximate temperature regions in which the high- and low-density and restrained forms of amorphous ice and the cubic and hexagonal crystalline states, respectively. T_g is the temperature of transition of glassy amorphous ice to a ultrasupercooled super-viscous liquid state.

First we must clarify the situation in regard to the desorption curves, in particular, with the origin of the first two low-temperature peaks. We did special studies which showed that they exist independently of whether the substrate is covered by an ASW film or is clean. We are inclined to the opinion, set forth in Ref. 30, that these two peaks reflect a process of desorption of nitrogen from the surface of the cryostat and partly from the surface of the ice. The first peak ($T_{\text{max}} \approx 26\ \text{K}$) corresponds to the desorption of nitrogen polylayers, and the second ($T_{\text{max}} \approx 34\ \text{K}$) is due to the desorption of a nitrogen monolayer. The rather sharp demarcation of these peaks attests to the determinate nature of the activation energies for desorption of a monolayer and poly-layers of nitrogen.

The third desorption peak, with maximum at $T_{\text{max}} \approx 42\ \text{K}$, is the result of the liberation of nitrogen from the sample. We assume that this process cannot be characterized in full measure as desorption (although we shall use this term below). Most likely the nitrogen molecules had been trapped by layers of ice during growth of the film, i.e., in our case the nitrogen molecules of the residual gases are immobilized in the water cryomatrix. Such a system is essentially metastable, as the maximum of the desorption corresponds to the very beginning of the low-temperature transformations in ASW.

Let us now turn to a direct analysis of the data presented in Fig. 4. We compare the variation of the IR spectrometer signal at a frequency of $3015\ \text{cm}^{-1}$ and the indications of a vacuum meter with the data of structural measurements^{1–3} in the form of the variation of the intensity of the diffraction

peaks due to the amorphous phase. It is seen that these results are in splendid agreement, so that one can reach the following conclusions, based on the data of Jenniskens and co-workers.

1. In the temperature interval from 16 K to 36–40 K our samples are found in the hda state. Further increasing the temperature to the interval 40–60 K is accompanied by a gradual transition from hda to lda. The very beginning of this transition corresponds to the onset of the desorption process ($T=36$ K), the maximum of which corresponds to a temperature of 42 K. Increasing the temperature further is accompanied by a gradual fall of the desorption peak, which is completed at $T\approx 63$ K, in agreement both with our IR measurements and with the data of Jenniskens. We shall show that the observed desorption process is due to the appearance of pores in the low-density amorphous water films, through which cryocooled nitrogen molecules pass out of the interior of the sample to its surface and are desorbed. The small minimum at $T=63$ K may be due to the circumstance that in the process of simultaneous formation of the pores and diffusion of nitrogen through them, a portion of the nitrogen is sorbed on the inner surface of these pores. When the transition from hda to lda at $T=70$ K is completed, an equilibrium state is reached between sorbent and sorbate.

2. As is seen in Fig. 4, in the temperature interval 70–120 K there are no clear signs of transformations in the ASW state. Meanwhile, there are some features that can be interpreted as a response to transformations in the layer. In particular, near 90 K the lower curve of the IR spectrometer signal begins to gradually fall, corresponding to a smooth shift of the stretching band absorption to lower frequencies. The same thing, but in a considerably sharper form, can be observed in Fig. 3. These data can be linked to the presence of a small maximum ($T=90$ K) in the data of Jenniskens. Furthermore, the desorption curves presented in Fig. 6 also have a pronounced maximum at these temperatures.

3. The temperature region near the glass transition temperature $T_g\approx 136$ K. In this range all of the parameters observed exhibit sharp variations. The indications of the IR spectrometer at frequency 3015 cm^{-1} decrease sharply, implying a substantial broadening and red shift of the stretching band of absorption, i.e., a sharp increase of the degree of hydrogen bonding.

The start of the glass transition unambiguously corresponds to the growth of the pressure in the chamber, which reaches a maximum at $T\approx 138$ K. This peak is most likely due to a sharp decrease of the degree of porosity of the ice at the transformation from ASW to the super-viscous liquid, which leads to crowding out of the nitrogen sorbed on the inner surfaces of the pores. The processes discussed for this temperature region are in splendid agreement with the data of Jenniskens.

4. It should be noted that, according to the IR spectrometer data, the process of transformation of the waveguide state to the quasi-liquid state has an obvious stepped character. In Fig. 4 we have noted this in a large number of experiments. This is demonstrated with particular clarity in the temperature interval from 146–150 K up to ≈ 165 K. Possibly this is due to the rather stable existence in this region of the super-viscous liquid phase^{3,31} with nuclei of the cubic

and hexagonal phases of ice “dissolved” in it.^{1,2} Growth of the cubic phase is slowed by the presence of the energetically more favorable but “supercooled” hexagonal nuclei. This is the state that Jenniskens^{1,2} defines as “restrained amorphous” (ra).

5. Above $T\approx 165$ K one observes a sharp transition which we interpret as a partial transformation of the ra state to the cubic modification of crystalline ice. This state remains practically unchanged up to a temperature $T\approx 180$ –185 K, and then sharp variations of the value of the IR spectrometer signal are observed upon further increase in temperature. The increase in the signal starts at temperatures from 180 to 185 K and reaches a maximum at 187 and 190 for the curves considered. Then a sharp drop is observed, followed by relative stabilization up to a temperature of around 200 K. At $T>200$ K the sample begins to evaporate. The observed process is accompanied by an increase in the pressure in the chamber, followed by a decrease.

The set of experimental data under discussion can be interpreted as follows. The inhomogeneous system consisting of amorphous and crystalline components has different equilibrium partial pressures. According to the data of Ref. 32, the activation energy for desorption of amorphous and crystalline cryocondensates of water are equal to 46.9 and 48.3 kJ/mole, respectively. Then the observed behavior of the warming curve is a consequence of recondensation of the amorphous component into the crystalline. Since the equilibrium pressure of the amorphous component is higher than that of the crystalline, this leads first to its evaporation, which is accompanied by both a decrease of the film thickness as an increase of the degree of its transparency (growth of the IR spectrometer signal). Sublimation of the molecules of the amorphous water causes an increase of the pressure in the chamber (the lower right-hand inset in Fig. 4). In view of the rather large dimensions of the chamber the process of evaporation of the amorphous component is separate in time from the process of its recondensation into the crystalline (apparently hexagonal) phase.

To check the ideas mentioned, we did a series of experiments with the KBr shielding slab (6 in Fig. 1) in place. It was assumed that in the closed substrate–slab space the processes of evaporation of the amorphous component and its

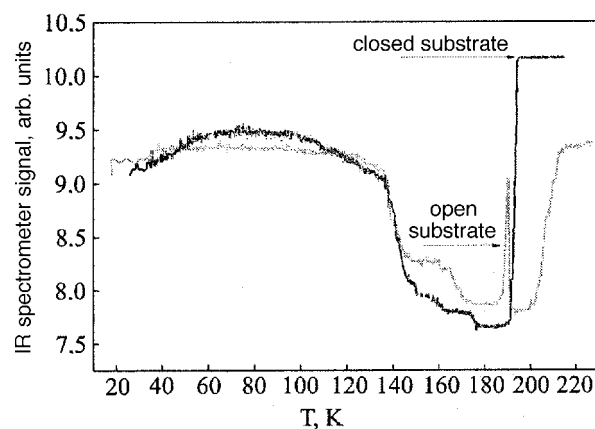


FIG. 5. Respectively of the IR spectrometer signal at frequency 3015 cm^{-1} in a situation with open and closed substrate. Film thickness $d=0.75\text{ }\mu\text{m}$, condensation temperature $T=16\text{ K}$, rate of condensation $V_c=0.5\text{ nm/s}$.

recondensation into the crystalline form will occur almost simultaneously. This, on the one hand, should prolong the processes of evaporation of the sample as a whole and, on the other hand, should cause the features in the temperature interval 180–200 K (Fig. 4) to vanish. The corresponding data are presented in Fig. 5. It is seen that our hypothesis about the recondensation peaks has been confirmed. Moreover, with the where covered, the stepped character of the transformations at temperatures above T_g becomes obvious. This is most likely due to the fact that for the small volume the film contains a sufficient quantity of matter to ensure an equilibrium value of the pressure of the gas phase over a wider temperature interval.

More-detailed studies were made of desorption processes in films of cryocondensates of water formed at different temperatures. The data of those studies can provide indirectly information about the structure of the film, including the state of its surface. Samples of equal thickness ($d = 0.75 \mu\text{m}$) were used. They were formed at the indicated temperatures, and then the shielding slab (6 in Fig. 1) was placed over the substrate, and in that state the sample was cooled to $T = 16 \text{ K}$. After stabilization of the temperature and a hold for 10 min the shielded substrate was removed, and the process of warming with simultaneous measurement of the temperature and pressure in the chamber was begun. The pumping down of the chamber was decreased enough that the initial pressure (10^{-7} torr) did not rise. When the temperature reached 165 K the pumping down of the chamber was shut off completely.

Figures 6 and 7 show the experimental data on the dependence of the pressure in the chamber (normalized according to the initial pressure $P = 10^{-7}$ torr) on the temperature of the use at different condensation temperatures. For comparison the figures also show the results of thermal desorption of a substrate free of cryocondensate. The data were grouped into two intervals of condensation temperatures.

The first interval (Fig. 6), 16–70 K, is characterized by the presence of four pronounced desorption peaks and one weak pressure increase. The first two maxima, at $T = 24$ and 34 K, correspond to desorption of surface poly- and monolayers of nitrogen. As we have said, these peaks are always

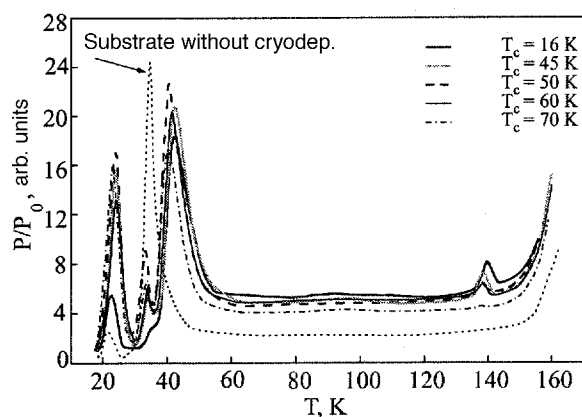


FIG. 6. Thermal desorption curves of ASW samples of thickness $d = 0.75 \mu\text{m}$, formed at temperatures in the interval 16–70 K, cooled to $T = 16 \text{ K}$, and warmed at a rate $V_{\text{ann}} \approx 0.03 \text{ K/s}$ in the interval 16–60 K and $V_{\text{ann}} \approx 0.01 \text{ K/s}$ at $T > 60 \text{ K}$.

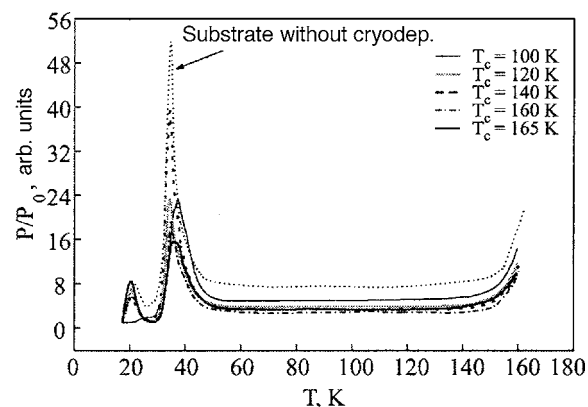


FIG. 7. Thermal desorption curves of ASW samples of thickness $d = 0.75 \mu\text{m}$, formed at temperatures in the interval 100–165 K, cooled to $T = 16 \text{ K}$, and warmed at a rate $V_{\text{ann}} \approx 0.03 \text{ K/s}$ in the interval 16–60 K and $V_{\text{ann}} \approx 0.01 \text{ K/s}$ at $T > 60 \text{ K}$. The thermal desorption curve of the clean substrate is also shown for comparison (it has been shifted upward by 4 arbitrary units).

present, even for experiments with a clean substrate. The third sharp peak, with maximum at $T = 42 \text{ K}$, corresponds to the process of nitrogen desorption through pores that arise as a result of a transition from the high-density to the low-density amorphous state. Here the desorption process reaches a maximum at the very beginning of that transition, which is indicative of a substantially unstable equilibrium between the nitrogen molecules and the hda matrix at these temperatures. Furthermore, one observes a weak shift of the desorption maximum to lower temperatures as the condensation temperature is increased. For example, at a condensation temperature $T_c = 16 \text{ K}$ the position of the maximum is determined by the temperature $T_{\text{max}} = 42.7 \text{ K}$, while at the same time, for a sample condensed at $T_c = 70 \text{ K}$, one has $T_{\text{max}} = 40.3$. As to the amplitude of the desorption peak, under the given conditions it varies only slightly in the direction of a decrease with increasing condensation temperature.

In the temperature interval 80–100 K the curves under discussion have a slight maximum, which might be taken to be measurement error if not for its regular appearance. Apparently, at these temperatures changes occur in ASW, which, meanwhile, do not have a noticeable influence on the degree of porosity. Here we know (Fig. 3) that the IR measurements at fixed frequency reveal characteristic and significant variations at these temperatures.

The pronounced maxima in the region $T \approx 140 \text{ K}$ are apparently due to a transition from the glassy ASW state to the super-viscous liquid state. Here one observes a correlation between the position of the maximum and the condensation temperature. The higher the condensation temperature of the films, the lower the temperature position of the desorption maximum. Here the start of the peak lies at the same temperature, 136 K, which corresponds to $T_g = 136 \text{ K}$. Furthermore, the condensation temperature $T = 70 \text{ K}$ is apparently the maximum for which a weak feature of the thermal desorption is observed at the glass transition temperature. Here the desorption peak at $T = 42 \text{ K}$, corresponding to an hda \rightarrow lda transition, is still significant.

To reveal the character of the behavior of the thermal desorption curve in the region of high sample condensation

temperatures, measurements were made at condensation temperatures in the interval 100–165 K. These data are presented in Fig. 7.

It is seen in the figure that there are no peaks corresponding to structural changes in the layer of water cryocondensate. The two peaks present correspond to desorption of polylayers and a monolayer of nitrogen from the surface of the cryostat and from the ice itself. True, it is seen that the position of the first peak is shifted to lower temperatures, its maximum at $T_{\max} \approx 20$ K as compared to $T_{\max} \approx 24$ K for the lower condensation temperature. Thus one can conclude that at condensation temperatures above ≈ 100 K the layers of solid water cannot restrain nitrogen molecules, neither by the cryotrapping mechanism nor by cryosorption.

One also notices the anomalously high amplitude of the desorption peak at $T=34$ K for the sample condensed at $T=140$ K, i.e., at the boundary of the glass transition. One of the explanations for this fact may be the following. If at a given temperature a quasi-liquid state forms on the substrate, then the penetration depth of the nitrogen molecules from the gas phase into the layer increases sharply owing to the significantly enhanced diffusion coefficient.³¹ On cooling these molecules, as it were, freeze into the subsurface layer, and on heating give a substantial addition to the desorption amplitude in comparison with the glassy and crystalline states of the samples at condensation temperatures above or below 140 K.

CONCLUSION

Our simultaneous IR spectrometric and thermal desorption measurements of thermally stimulated processes in amorphous solid water and their comparison with the data of Jenniskens and co-workers permit the following conclusions.

1. The temperature interval 12–36 K is the existence region of the high-density form of ASW (hda). In an absolute majority of the experiments done the features that are characteristic for this state of amorphous matter appear in the IR spectra and warming curves. The transition of the high-density amorphous ice to the low-density amorphous state (lda) begins at $T \approx 39$ K and is completed in the temperature interval 60–70 K. This process is accompanied by the formation of pores. Analysis of the thermal desorption data suggests that the process of pore formation reaches its maximum intensity at a temperature of ≈ 42 K. Furthermore, a sharp maximum of the desorption peak at that temperature attests to the circumstance that these pores have a predominant direction perpendicular to the film, ensuring the simultaneous start of the desorption processes over the whole thickness of the sample.

2. The transition from hda to lda is accompanied by a sharp shift of the stretching band absorption peak to lower frequencies (Fig. 2a) and of the peak of librational oscillations (Fig. 2b) to higher frequency. This attests to an increase of the degree of order in the system. The cause of this is the nonuniform tuning of the sample as a whole, and the process of pore formation, which leads to an increase of the number of surface molecules and, as a consequence, to a larger degree of their ordering in comparison with molecules lying in the interior of the sample. This conclusion agrees with the

results of a majority of studies, in particular, those presented in Ref. 9.

3. The temperature existence region of the low-density form of ASW is not completely determined. For different samples condensed under experimentally monitored constant conditions one observes features that may attest to transformations in the layer. Here the manifestation of these transformations can occur at surface temperatures. In our view, this is due to stochastic processes of formation of amorphous solid water at low temperatures, at which the establishment of a relation between the cubic and hexagonal nuclei of the crystalline phase is of an indeterminate character. Meanwhile, our simultaneous IR spectrometric and thermal desorption studies suggests the conclusion that in the temperature interval 80–100 K the transition from the low-density form of ASW to, most likely,^{1–3} the restrained amorphous state.

4. In accordance with our data it can be stated that the temperature of the transition from the glassy amorphous ice to the super-viscous liquid state is $T_g = 137 \pm 2$ K. Further increase of the temperature leads to transformations in the layer which have a stepped character. This may be due to competing processes of crystallization as a result of the growth of the cubic and hexagonal nuclei and also to direct crystallization of the super-viscous liquid formed at T_g and existing together with the crystalline phase up to temperatures of the order of 200 K.^{3,9}

5. Our studies have revealed an anomalous character of the behavior of the samples at temperatures preceding sublimation. This consists in a jumplike behavior of the warming curve, which is accompanied by an extremum of the value of the pressure in the chamber. These experimental data confirm the point of view expressed in Refs. 3, 9, 31, and 32. We are talking about the idea that a multicomponent system consisting of amorphous and crystalline components at a fixed temperature should have different values of the equilibrium pressures of the gas phase, corresponding to partial activation energies of sublimation, since the value of the activation energy of the amorphous form of ice ($E_a = 46.9$ kJ/mole) is lower than the corresponding values for the crystalline modifications ($E_a = 48.3$ kJ/mole),³ and this leads to the situation that at high temperatures amorphous water evaporates at an earlier stage and then recondenses on the crystalline components into crystalline form. The data of Figs. 4 and 5 clearly confirm such a mechanism.

6. A sharp peak of the desorption curve with maximum at $T=42$ K (Fig. 6) corresponds to a process of nitrogen desorption through pores that arise as a result of a transition from the high-density to the low-density amorphous state. The fact that the desorption process reaches a maximum at the very beginning of this transition normalized that the equilibrium between nitrogen molecules and the hda matrix at these temperatures is essentially unstable. Furthermore, one observes a weak shift of the desorption maximum to lower temperatures as the condensation temperature increases. For example, at a condensation temperature $T_c = 16$ K the position of the maximum is given by the temperature $T_{\max} = 42.7$ K, while for a sample condensed at $T_c = 70$ K the temperature $T_{\max} = 40.3$ K.

At condensation temperatures above 90–100 K (Fig. 7) the formation of a film of cryocondensate of water is not accompanied by the trapping of gaseous nitrogen. This is indicated by the absence of desorption peaks both in the region of polyamorphic transformations and at the glass transition temperatures. One can conclude that at these temperatures the cryocondensates of water grow in the form of smooth films with a small pore content.

7. We have found that a sample condensed at $T=140$ K, i.e., at the boundary of the glass transition, has an anomalously high desorption peak corresponding to desorption of a nitrogen monolayer. We consider this to be possible confirmation of the existence of a liquid state of water at these temperatures. If that is the case, then the penetration depth of the nitrogen molecules from the gas phase into the layer is sharply increased owing to the significantly higher diffusion coefficient of nitrogen in the layer. On cooling these molecules freeze into a subsurface layer, and on heating they give a substantial addition to the amplitude of desorption in comparison with the glassy and crystal states of the sample at condensation temperatures above or below 140 K.

^aE-mail: drobyshev@kazsu.kz

¹P. Jenniskens and D. Blake, *Science* **265**, 5, 753 (1994).

²P. Jenniskens and D. Blake, *Astrophys. J.* **473**, 1104 (1996).

³P. Jenniskens, S. F. Banham, D. F. Blake, and M. R. S. McCoustra, *J. Chem. Phys.* **107**, 1232 (1997).

⁴V. F. Petrenko and R. W. Whitworth, *Physics of Ice*, Oxford University Press, New York (1999).

⁵P. J. Debenedetti, *J. Phys.: Condens. Matter* **15**, 1669 (2003).

⁶E. F. Burton and W. F. Oliver, *Nature (London)* **135**, 505 (1935).

⁷S. A. Rice and A. G. Sceats, *J. Chem. Phys.* **69**, 3468 (1978).

⁸A. H. Narten, C. G. Venkatesh, and S. A. Rice, *J. Chem. Phys.* **64**, 1106

(1976).

⁹Ph. Parent, C. Laffon, C. Mangeney, F. Bournel, and M. Tronc, *J. Chem. Phys.* **117**, 10842 (2002).

¹⁰C. A. Angell, *Science* **267**, 1924 (1995).

¹¹P. J. Debenedetti, *Nature (London)* **392**, 127 (1998).

¹²G. P. Johari, A. Hallbrucker, and E. Mayer, *Science* **273**, 90 (1996).

¹³B. Guillot and Y. Gussani, *J. Chem. Phys.* **120**, 4366 (2004).

¹⁴C. A. Tulk, C. J. Benmore, J. Urquidi, D. D. Klug, J. Neufeind, B. Tomberli, and P. A. Egelstaff, *Science* **297**, 1320 (2002).

¹⁵A. Hallbrucker, E. Mayer, and G. P. Johari, *J. Phys. Chem.* **93**, 4986 (1989).

¹⁶C. A. Tulk, D. D. Klug, R. Brandenhorst, P. Sharp, and J. A. Ripmeester, *J. Chem. Phys.* **109**, 8478 (1998).

¹⁷A. Hallbrucker, E. Mayer, and G. P. Johari, *Philos. Mag. B* **60**, 179 (1989).

¹⁸C. A. Angell, *Science* **267**, 3, 1924 (1995).

¹⁹Y. Yue and C. Angell, *Nature (London)* **427**, 717, (2004).

²⁰G. P. Johari, *J. Chem. Phys.* **119**, 2935 (2003).

²¹N. J. Sack and R. A. Baragiola, *Phys. Rev. B* **48**, 9973 (1993).

²²A. S. Drobyshev and T. A. Prokhotseva, *J. Low Temp. Phys.* **119**, 431 (2000).

²³A. S. Drobyshev, N. V. Atapina, D. N. Garipogly, S. L. Maksimov, and E. A. Samyshkin, *Fiz. Nizk. Temp.* **19**, 567 (1993) [*Low Temp. Phys.* **19**, 404 (1993)].

²⁴A. S. Drobyshev, D. N. Garipogly, S. L. Maksimov, and E. A. Samyshkin, *Fiz. Nizk. Temp.* **20**, 600 (1994) [*Low Temp. Phys.* **20**, 475 (1994)].

²⁵M. P. Malkov, *Handbook of Physico-Technical Principles of Cryogenics* [in Russian], Energiya, Moscow (1973).

²⁶N. J. Sack and R. A. Baragiola, *Phys. Rev. B* **48**, 9973 (1993).

²⁷A. Kouchi, *J. Cryst. Growth* **99**, 1220 (1990).

²⁸G. A. Kimmel, K. P. Stevenson, Z. Dohnalek, R. S. Smith, and B. D. Kay, *J. Chem. Phys.* **114**, 5295 (2001).

²⁹A. Drobyshev, A. Aldiyarov, D. Zhimagaliuly, V. Kurnosov, and N. Tokmoldin, *Fiz. Nizk. Temp.* **33**, 479 (2007) [*Low Temp. Phys.* **33**, 355 (2007)].

³⁰G. A. Kimmel, Z. Dohnalek, K. P. Stevenson, R. S. Smith, and B. D. Kay, *J. Chem. Phys.* **114**, 5284 (2001).

³¹R. S. Smith and B. D. Kay, *Nature (London)* **398**, 788 (1999).

³²R. J. Speedy, P. J. Debenedetti, R. S. Smith, C. Huang, and B. D. Kay, *Chem. Phys.* **105**, 240 (1996).

Translated by Steve Torstveit